Journal of Thermal Analysis and Calorimetry, Vol. 93 (2008) 3, 907–914

STUDY BY THERMAL METHODS ON SOME NEW CYCLIC YLIDES AND DERIVATIVES

C. Moldoveanu[1], *Lucia Odochian*[1], *I. Mangalagiu*[1], *M. Dumitraş*[1*] *and N. Apostolescu*[2]

[1]'Al. I. Cuza' University, Faculty of Chemistry, 11 Carol I Bd, Iassy, Romania
[2]'Gh. Asachi' University, Faculty of Chemical Engineering, 71A D. Mangeron Bd, Iassy, Romania

The study is devoted to the characterization by TG, DTG, DTA, both in air and N_2 atmosphere, of three cyclic ylides as well as two spirane derivatives, to the purpose of elucidating the correlation between structure, thermostability and thermal degradation mechanism. Thermal analysis data indicated that the degradation mechanism is characteristic for every sample, and the consequences of structural peculiarities are discussed. The thermostability series of the samples is correlated to their structure. The quantitative TG-DTG-DTA analysis allowed some considerations on the thermal degradation mechanism, subsequently confirmed by mass spectrometry. The melting points obtained by DTA and Boetius measurements along with the initial degradation temperatures from TG-DTG-DTA curves indicates the temperature range for the use and storage of these compounds, considering that some derivatives of cyclic ylides show biological activity and potential medical applications.

Keywords: *cyclic ylides, DTA, DTG, mass spectrometry, spiranes, TG, thermal analysis*

Introduction

The cycloaddition reactions, belonging to the pericyclic reactions, are particularly important in organic chemistry [1, 2] due to their numerous theoretical and practical applications in virtue of the biological activity shown by some derivatives with potential medical applications [3–8].

Following our previous studies in the field the present paper deals with the characterization of three cyclic ylides: 3-(4-(4-chlorophenyl)pyrimidin-1-ium-1-yl)-2,5-dioxotetrahydrofuran-3-ide (**a**); 3,4-dichloro-4-(4-(4-chlorophenyl)pyrimidin-1-ium-1-yl)-2,5-dioxotetrahydrofuran-3-ide (**b**); 4-(4-(4-chlorophenyl)pyrimidin-1-ium-1-yl)-3-methyl-2,5-dioxote-trahydrofuran-3-ide (**c**), as well as two spirane derivatives: 3-(4-chlorophenyl)-6,7-dicarboxy-N-phenyl-imido-8-spiro-(3'-tetrahydropyrrolo-N-phenyl-2'5'-dione)-5,6,7,8-tetrahydropyrrolo[1,2-c]pyrimidine (**d**); 3-(4-chlorophenyl)-6,7-dicarboxy-N-ethylimido-8-spiro-(3'-tetrahydropyrrolo-N-ethyl-2'5'-dione)-5,6,7,8-tetrahydropyrrolo[1,2-c] pyrimidine (**e**), by TG, DTG, DTA thermal analyses [9, 10] both in air and N_2 atmosphere, coupled with mass spectrometry measurements in order to elucidate the correlation between structure, thermostability and degradation mechanism.

The characterization by thermal methods, extensively used in the literature for both natural and synthetic compounds [11–14], states precisely the optimum temperature range for using and storing these compounds and thermostability series is correlated with their structure.

The quantitative analysis by TG-DTG-DTA [15, 16] in air and N_2 atmosphere allowed a discussion on the thermal degradation mechanism. Similarities were noticed for the compounds **a**, **b**, **c** while the compounds **d**, **e** showed specific and complex degradation mechanism greatly influenced by their substituents.

The conclusions on the thermal degradation mechanisms obtained by TG-DTG-DTA analyses were supported by the mass spectra obtained under chemical ionization conditions.

The melting points estimated from DTA data [17], in air and in N_2 atmosphere, were in good agreement with those found by the Boetius method.

Experimental

Materials

The structures of the cyclic ylides and spirane derivatives under study, their molecular formula and IUPAC denominations, molecular masses and melting points measured by the Boetius method are presented in Scheme 1.

The synthesis of these compounds and their characterization by elemental analysis and NMR spectral measurements were described in a previous paper [18]. The synthesis of the spirane compounds **d**, **e** from the cyclic ylides similar to **a**, **b** and **c** confirms the cyclic ylidic structure of the last.

The cyclic ylides were separated from CH_2Cl_2 (*b.p.*=39–40°C) and the spirane compounds synthe-

* Author for correspondence: mihai.dumitras@uaic.ro

1388–6150/$20.00

Akadémiai Kiadó, Budapest, Hungary
Springer, Dordrecht, The Netherlands

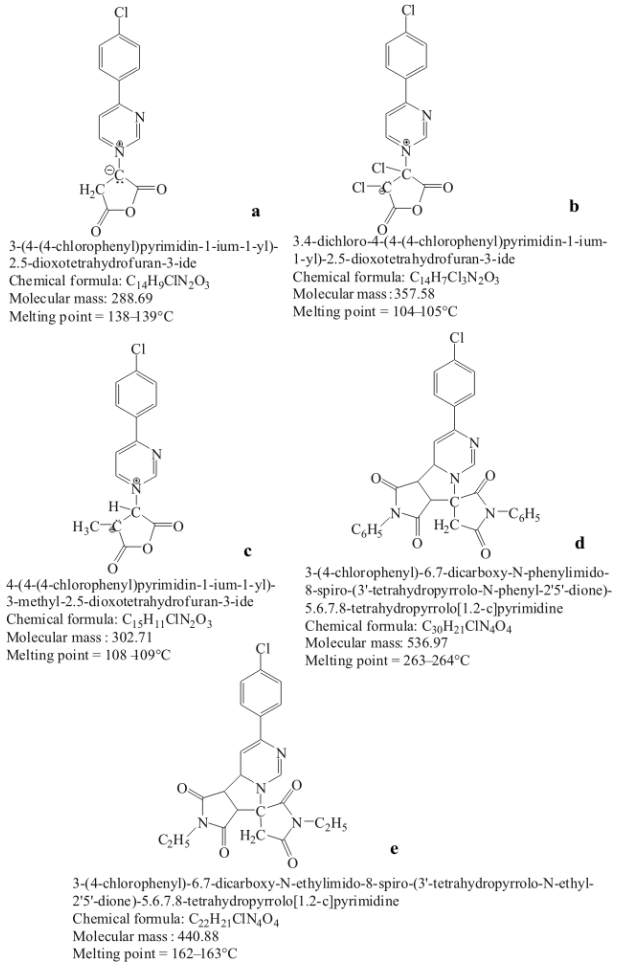

Scheme 1 Samples under study (structure, molecular mass and melting points)

sized in acetic acid (*b.p.*=117–118°C) were recrystallized from $C_2H_5OC_2H_5$ (*b.p.*=34–35°C).

Methods

Thermal analysis

The thermogravimetric (TG) and differential thermal analysis (DTA) were performed by using a Perkin-Elmer Pyris Diamond TG/DTA thermobalance which records simultaneously *T*, TG and DTA curves. The DTG curves were obtained by numerical differentiation of the TG curves. The working conditions were as follows: sample mass 12 mg, heating rate 10°C min^{-1}, temperature range 30–900°C in N_2 stream and in air (80 mL min^{-1}).

Mass spectrometry

The mass spectra were recorded on a GCMS Shimadzu QP2010 mass spectrometer with DI (direct inlet) and CI (chemical ionization). Reagent gas was CH_4.

Results and discussion

The TG and DTG curves obtained in air and in N_2 with the samples under study are depicted in Figs 1 a–e.

Analysis of the TG and DTG curves of the samples indicates the degradation mechanism in both air and N_2 atmosphere under working condition to be complex and specific to every sample. Within the 30–450°C range all the investigated samples showed a similar behavior in both air and N_2 while between 450–700°C significant differences were noticed in the degradation mechanisms in air and N_2. The characteristic temperatures corresponding to the degradation stages, mass losses (w_∞%) and the remaining residue are listed in Table 1.

During the first stage, between 62–175°C, the solvent remaining after sample purification [16] is eliminated, with a 0.3–5% mass loss, every sample showing the same mass loss in both air and N_2.

Stages II–VI, between 105–646°C, correspond to sample degradation in air and N_2 atmosphere. Sample **a** exhibits four degradation stages in air, with no remaining residue, while in N_2 atmosphere degradation occurs in three stages, with a black crystalline residue (9.6%). The temperatures characteristic of the common stages (stages II–IV) are the same for the degradations in air and in N_2 atmosphere.

Sample **b** shows six degradation stages in air and five in N_2. The temperatures characteristic to the stages II–V are the same both in air and in N_2, and in N_2 a crystalline black residue (20.3%) is obtained. With the sample **c** two major significant stages were noticed in both air and N_2, with the same temperature ranges, an additional stage for degradation in air and a small amount of residue in N_2 (3.5%) being noticed.

The spiranes **d** and **e**, as derivatives of the cyclic ylides, show several degradation stages within different temperature domains which differ also from those of the samples **a**, **b** and **c**.

Thus the sample **d** is thermally degraded into three stages (II–IV) in both air and N_2 within the same temperature ranges for the stages II–III, when an amorphous black residue is obtained in N_2 (23.7%), while sample **e** is degraded into two stages (II–III) within the same temperature ranges in the II^{nd} stage, an amorphous black residue resulting after degradation in N_2 (7.7%).

The thermostability of the samples expressed by the T_i – initial degradation temperature in air and in N_2 (Table 1) leads to the following series correlated with the chemical structures of the compounds under study: **e**>**d**>**a**>**c**>**b**.

Thus, the spiranes **d** and **e** are much more stable than the cyclic ylides, explained by the fact that they do not show electrical charges while the last have both negative and positive charges (2). The two

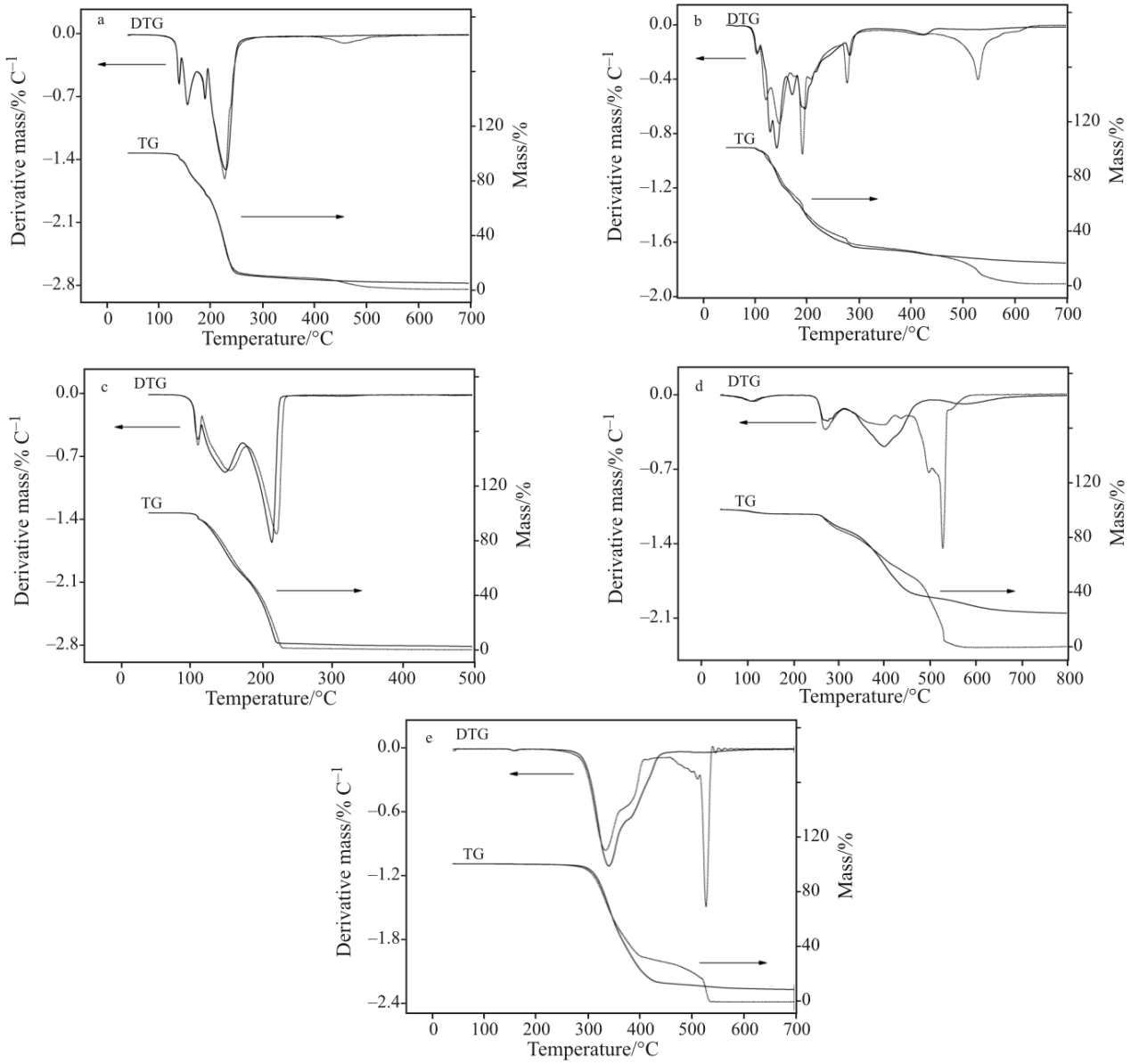

Fig. 1 TG and DTG curves for a – ylide **a**, b – ylide **b**, c – ylide **c**, d – spirane **d** and e – spirane **e** (— – N_2, --- – air)

spiranes differ in the nature of the group bound on the nitrogen atom (Scheme 1) (R–Ph in the compound **d** and R–Et in the compound **e**). Since the ethyl group is less bulky than the phenyl group the sterical hindrance in **e** is lower and consequently the compound **e** is more stable than **d**.

The ionic intermediates are well known (2) to be increasingly stable with decreasing charge. The cyclic ylides **a**, **b** and **c** differ by the nature of the substituents on the anhydride ring carrying negative charges (the compound **b** differs from **e** by the two chlorine atoms while **c** carries a CH_3 group unlike compound **a**).

The electron-releasing inductive effect of the $–CH_3$ group results in an increased electronic density on the ylidic carbon atom leading to the stability decrease of **c** as compared to **a**.

The low stability of ylide **b** is caused by the two chlorine atoms in its structure acting by both significant steric hindrance in the molecule and stabilization effect on the anionic fragments formed during degradation.

The DTA curves of the samples **a**, **b**, **c**, **d** and **e** recorded both in air and N_2 atmosphere are illustrated in Fig. 2, where the same major degradation steps as in TG-DTG curves are made evident. Within 92–400°C range the degradation steps are endothermal both in air and N_2 and further, between 400–700°C, the degradation is exothermal in air and absent in nitrogen.

In Table 2 the characteristic temperatures of the degradation steps from DTA, their thermal nature and the areas of the normalized exothermal peaks are listed (Table 2).

Table 1 Characteristic temperatures (°C) and mass loss (%) from DTG in air and N_2

Stage		Sample									
		a		**b**		**c**		**d**		**e**	
		air	N_2	air	N_2	air	N_2	air	N_2	air	N_2
Stage I	T_i	110	110	80	79	85	85	62	62	142	142
	T_m	138	138	99	101	109	109	110	110	160	156
	T_f	143	143	105	106	115	115	168	168	172	172
	w_∞	5	4.8	2.6	2.6	5.5	5.4	3.2	3.2	0.3	0.4
Stage II	T_i	143	143	105	106	115	115	230	230	262	262
	T_m	155	155	117 142	125 138	147	155	269	269	334	341
	T_f	173	173	163	156	172	179	310	310	430	445
	w_∞	16.3	16.2	29.5	28.8	39.5	38.2	13.2	11.3	70.5	87.2
Stage III	T_i	173	176	163	156	172	179	310	310	460	476
	T_m	188	188	172	168	214	220	397	397	530	526
	T_f	194	194	177	177	231	237	447	502	543	675
	w_∞	10.66	10.5	5.1	9.3	51.6	52.9	30.7	50.1	29.2	4.7
Stage IV	T_i	194	194	177	177	231	–	447	502	–	–
	T_m	226	228	192	187	–	–	526	576	–	–
	T_f	295	298	196	196	700	–	586	800	–	–
	w_∞	57	58.9	12	10.5	3.1	–	52.9	11.7	–	–
Stage V	T_i	377	–	352	352	–	–	–	–	–	–
	T_m	459	–	421	421	–	–	–	–	–	–
	T_f	524	–	445	445	–	–	–	–	–	–
	w_∞	11.04	–	30.2	28.5	–	–	–	–	–	–
Stage VI	T_i	–	–	445	–	–	–	–	–	–	–
	T_m	–	–	527	–	–	–	–	–	–	–
	T_f	–	–	647	–	–	–	–	–	–	–
	w_∞	–	–	20.6	–	–	–	–	–	–	–
Residue/%		–	9.6	–	20.3	–	3.5	–	23.7	–	7.7

The temperature intervals of the degradation steps in air and nitrogen are close to those found from TG-DTG for the steps that could be separated in DTA.

On the basis of initial temperatures from DTA for the degradation in air and N_2 the thermostability of the sample obeys the same series as with TG-DTG: **e**>**d**>**a**>**c**>**b**.

The first stage, corresponding to the solvent elimination, is an endothermal process. This stage overlaps with the sample melting. These two processes are well separated only when the difference between the solvent vaporization temperature and the sample melting point is high enough, as with sample **d**. With the samples **b** and **c** two maxima, not very well separated, are noticed in the first endothermal peak, unlike the samples **a** and **c** where they are not observed. A clear situation is in case of sample **e**

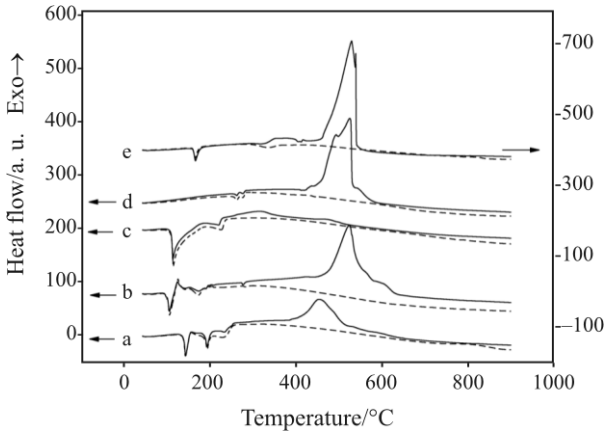

Fig. 2 DTA curves for samples **a**, **b**, **c**, **d** and **e** (— – air, --- – N_2)

Table 2 Characteristic temperatures (°C) and peak area from DTA in air and N_2

Stage		Sample									
		a		**b**		**c**		**d**		**e**	
		air	N_2	air	N_2	air	N_2	air	N_2	air	N_2
Stage I	T_i	120	120	89	89	94	94	246	245	148	150
	T_m	141	141	95	95	110	111	262	262	164	162
	T_f	154	154	97	97	186	192	267	269	183	182
		endo	endo	endo	endo	endo	endo	endo	endo	endo	endo
Stage II	T_i	154	154	97	97	186	191.8	267	269	287	281
	T_m	166	166	103.5	104	217	221	274	273	319	335
	T_f	174	174	123	123	230	240	285	284	354	424
		endo	endo	endo	endo	endo	endo	endo	endo	endo	endo
Stage III	T_i	174	174	123	123	230	–	420	–	445	–
	T_m	191	191	139	139	316	–	491 524	–	534	–
	T_f	215	207	150	150	357	–	353	–	454	–
		endo	endo	endo	endo	endo	–	exo	–	exo	–
Stage IV	T_i	215	207	150	150	357	–	–	–	–	–
	T_m	230	226	172	127	467	–	–	–	–	–
	T_f	259	267	201	201	515	–	–	–	–	–
		endo	endo	endo	endo	exo	–	–	–	–	–
Stage V	T_i	259	–	271	274	–	–	–	–	–	–
	T_m	453	–	275	281	–	–	–	–	–	–
	T_f	524	–	285	295	–	–	–	–	–	–
		exo	–	endo	endo	–	–	–	–	–	–
Stage VI	T_i	–	–	445	–	–	–	–	–	–	–
	T_m	–	–	523	–	–	–	–	–	–	–
	T_f	–	–	580	–	–	–	–	–	–	–
		–	–	exo	–	–	–	–	–	–	–
Peak area/a. u.		A_V 79.6	–	A_{VI} 172.3	–	A_{III+IV} 29.6	–	A_{III} 247.6	–	A_{III} 378.2	–

where the solvent content is low (0.3%) so that the melting endothermal peak is clearly made evident, the sample mass being constant.

The melting points of the samples **a**, **b**, **c**, **d** and **e** were estimated from the temperatures corresponding to the peak maximum in DTA [19].

The melting points from DTA in air and N_2 are listed in Table 3 in comparison with those measured with the Boetius microscope.

The mass losses in the degradation stage in N_2 atmosphere (Table 1) correlated with the normalized areas of the exothermal peaks in DTA (Table 2) affords a discussion on the thermal degradation mechanism of the samples. Thus, in Table 4 the normalized areas of the exothermal stages from DTA, the corresponding mass losses and residue resulting by thermal degradation in N_2 atmosphere are listed for the samples under study. It can be noticed that with the samples **a**, **b** and **c** the amount of residue resulting by degradation in N_2 is equal to the mass loss in the final stage of thermooxidative degradation.

Table 3 Melting points (°C) from DTA in air and N_2, and from Boetius method

Sample	DTA/°C		Boetius method/°C
	Air	N_2	
a	141	141	138–139
b	104	104	104–105
c	110	111	108–109
d	262	262	263–264
e	164	162	162–163

The normalized area ratio, A_b/A_a, is also equal to the residue ratio, R_b/R_a, for the thermal degradation in N_2 atmosphere: A_b/A_a=2.16, R_b/R_a=2.11.

The stages of the exothermal degradation in air of the samples **a**, **b** and **c** represents the burning of the resulting residue. The residue burning proceeds over the same temperature range for the three samples and the thermal effect is directly proportional to the mass of burning substance leading to the conclusion that the residue composition is the same in the three cases.

The C_{ylidic}–N bond in the cyclic ylides **a**, **b** and **c** is the weakest since for the N–ylides there is not possible to formulate stable structures of ylene type as with the P– and S–ylides. These labile bonds were made evident with the ylide **a** by the hydrolysis at both low and high temperature when the 4-(4-chlorophenyl)-pyridine resulting by the breaking of the C_{ylidic}–N bond [18] was separated. Consequently, the cyclic ylides **a**, **b** and **c** are expected to be thermally degraded into two major processes: first, the anhydride ring is degraded followed by the degradation of the pyrimidine ring since the first is less stable.

In Table 5 the experimental mass losses (from TG-DTG curves) corresponding to the two processes are presented. As expected from the above discussion, the theoretical and experimental values are close, showing small differences since the degradation stages are not well defined.

Table 4 Normalized exothermal peak area and the corresponding mass losses in air, respectively the residue in N_2

Sample	Peak area/ mm^2	w_∞/% (in air)	Residue/% (in N_2)
a	79.6	11.04	9.6
b	172.3	20.06	20.3
c	29.6	3.10	3.5
d	247.6	52.90	23.7
e	378.2	29.20	7.7

$$\frac{A_b}{A_a}=\frac{172.3}{79.6}=2.16;\ \frac{R_b}{R_a}=\frac{20.3}{9.6}=2.11;\ \frac{A_c}{A_a}=\frac{29.6}{79.6}=0.37;\ \frac{R_c}{R_a}=\frac{3.5}{9.6}=0.36$$

The samples **d** and **e** do not show correlations similar to those of the samples **a**, **b** and **c**, indicating a more complex degradation mechanism, the resulting residue being probably a thermostable resin.

The thermal degradation mechanism as proposed from the TG-DTG-DTA data is confirmed by the mass spectra recorded under the conditions of chemical ionization with CH_4 as an ionization gas. The mass spectra of the samples **a**, **b** and **c** are depicted in Figs 3a–c.

As made evident in Fig. 3 the main fragmentation reaction in the compounds **a**, **b** and **c** occurs at the

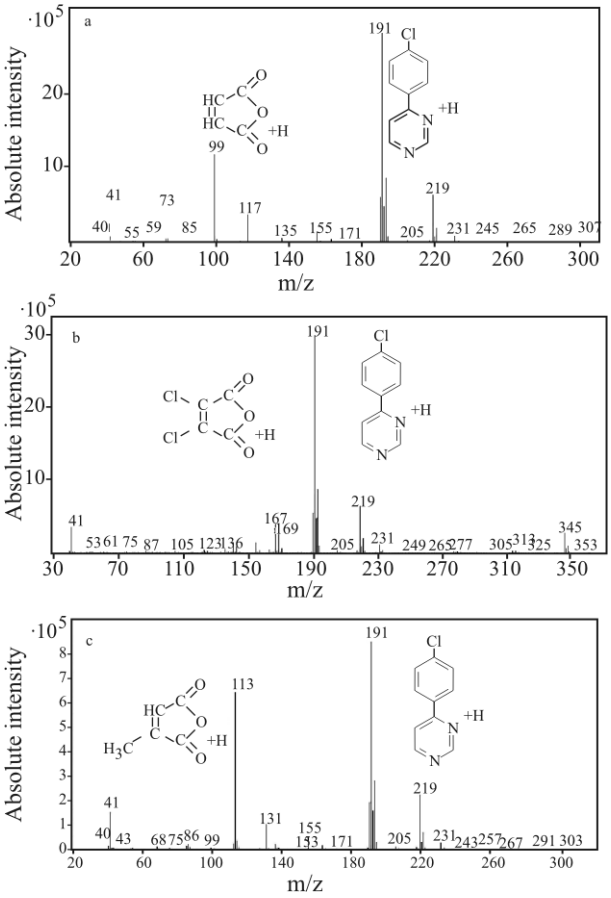

Fig. 3 Mass spectra of a – ylide **a**, b – ylide **b** and c – ylide **c**

Table 5 Theoretical and experimental mass losses (%) for the thermal degradation processes of the samples **a**, **b** and **c**

Process		Sample					
		a		b		c	
		$w_{\infty t}$	$w_{\infty exp}$	$w_{\infty t}$	$w_{\infty exp}$	$w_{\infty t}$	$w_{\infty exp}$
Process I Degradation of the anhydride ring	Stage	–	II+III	–	II+III+IV	–	II
		33.96	28.24	46.69	48.86	33.06	41.10
Process II Degradation of the pyrimidine ring	Stage	–	IV+V (air) IV+R (N_2)	–	V+VI (air) V+R (N_2)	–	III+IV (air) III (N_2)
		66.04	71.86	53.31	51.14	69.94	58.9

C_{ylidic}–N bond which would explain the occurrence of the main peak at *m*/*z*=191 (100%) corresponding to the pyrimidine ring. The same fragmentation is responsible for the signal, *m*/*z*=99 (42.61%) with the sample **a**, at *m*/*z*=267 (13.23%) with the sample **b** and at *m*/*z*=167 (13.23%) with the sample **c** corresponding to the anhydride rings, which confirms the mechanism advanced by means of TG-DTG-DTA for the samples **a**, **b** and **c**, described in Scheme 2.

Unlike the mass spectra of the ylides **a**, **b** and **c**, the mass spectra of the spiranes **d** and **e** do not indicate the splitting of the C–N bond as the main fragmentation since the corresponding signal *m*/*z*=191 is not anymore the main peak. In these two cases it has lower intensity, of 11.4 and 13.45% with the spiranes **d** and **e**, respectively (Figs 4a and b).

The fragmentations of the spiranes are much different from those of the ylides, indicating a much more complex degradation mechanism. The cross-linking tendency of spiranes can be noticed in the mass spectrum of the spirane **e**, where the intensity of the signal from higher *m*/*z* values (460) increases with time, from 6.44% at 5.9 min to 100% at 7.5 min. This confirms the formation of a thermally stable residue by cross-linking.

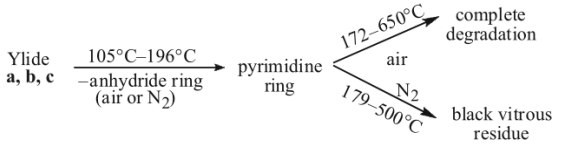

Scheme 2 Thermal degradation mechanism of the cyclic ylides

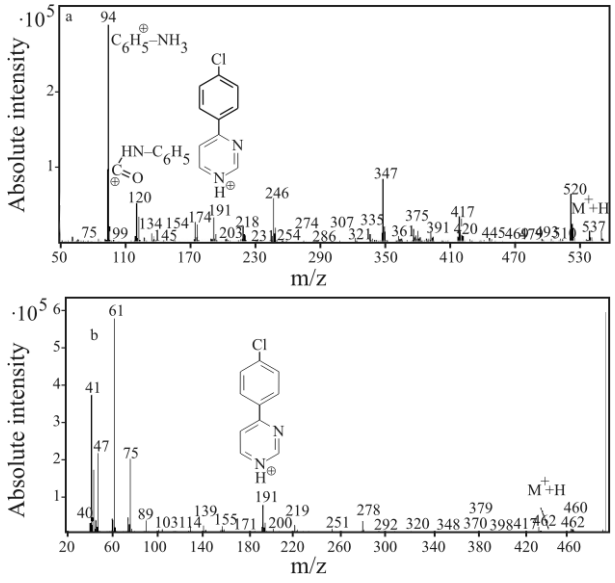

Fig. 4 Mass spectra of a – spirane **d** and b – spirane **e**

Conclusions

The analysis of TG-DTG curves for the samples under study indicates a complex degradation mechanism. For the cyclic ylides, a similar behavior can be noticed. No similarities can be observed with the spirans, as a consequence of the influence of structural dissimilarities and of the nature of substituents.

The thermostability of the samples estimated from the initial degradation temperature in DTG and DTA is expressed by the following series: **e**>**d**>**a**>**c**>**b**. The thermostability is correlated to the chemical structure, and the temperature domains proper for their use are ascertained.

The DTA analysis confirmed the degradation steps and their thermal nature as found by TG-DTG and allowed the estimation of the melting point, in very good agreement with the values measured by the Boetius method.

Quantitative TG-DTG-DTA analysis for the degradation in air and N_2 allowed a degradation mechanism to be advanced for the ylides **a**, **b** and **c**, supported by mass spectrometry. First, the ylidic C–N bond is split and the anhydride ring is degraded, followed by the degradation of the pyrimidine ring, leading to the formation of a thermostable residue in N_2 atmosphere.

For the spiranes (samples **d** and **e**) these stages were not identified, and the degradation mechanism is more complex and characteristic for every sample.

References

1 I. Zugravescu and M. Petrovanu, N-ylid chemistry, McGrow Hill, London 1976.
2 I. Zugravescu and M. Petrovanu, Cycloaditii 3-2 dipolare, Ed. Acad. Romane, Bucureşti 1987, p. 160.
3 M. Caprosu, M. Andrei, G. Mangalagiu, M. Petrovanu and I. Mangalagiu, Arkivoc, (2001) 1.
4 I. Mangalagiu, M. Ungureanu, G. Mangalagiu, G. Grosu and M. Petrovanu, Ann. Pharmacceutiques Fr., 56 (1998) 181.
5 G. Mangalagiu, M. Ungureanu, G. Grosu, I. Mangalagiu and M. Petrovanu, Ann. Pharmacceutiques Fr., 59 (2001) 139.
6 M. Ungureanu, C. Moldoveanu, A. Polata, G. Drochioiu, M. Petrovanu and I. Mangalagiu, Ann. Pharmacceutiques Fr., 64 (2006) 287.
7 I. M. Risca, G. Zbancioc, C. Moldoveanu, G. Drochioiu and I. Mangalagiu, Roum. Biotech. Letters, 11 (2006) 2563.
8 C. Moldoveanu and I. Mangalagiu, Helv. Chim. Acta, 88 (2005) 2747.
9 C. Vasile, E. M. Calugaru, A. Stoleriu, M. Sabliovschi and E. Mihai, Comportarea termica a polimerilor, Ed. Acad. Romane, Bucureşti 1980, p. 87.

10 E. Segal and D. Fatu, Intoducere in cinetica neizoterma, Ed. Acad. Romane, Bucureşti 1983, p. 15.
11 D. N. Sorensen, A. P. Quebral, E. E. Baroody and W. B. Sanborn, J. Therm. Anal. Cal., 85 (2006) 151.
12 C. D. Silva Marta, J. R. Botelho, M. M. Conceillo, B. F. Lira, M. A. Coutinho, A. F. Dias, A. G. Souza and P. F. A. Filho, J. Therm. Anal. Cal., 79 (2005) 277.
13 G. Bannach, E. Schnitzler, F. O. Treu, V. H. S. Utuni and M. Ionashiro, J. Therm. Anal. Cal., 83 (2006) 233.
14 G. Q. Zhong, S. R. Luan, P. Wang, Y. C. Guo, Y. R. Chen and Y. Q. Jia, J. Therm. Anal. Cal., 86 (2006) 775.
15 L. Odochian, J. Thermal Anal., 45 (1995) 1437.
16 L. Odochian, V. Dulman, M. Dumitras and A. Pui, J. Therm. Anal. Cal., 89 (2007) 652.
17 M. Dumitras and L. Odochian, J. Therm. Anal. Cal., 69 (2002) 599.
18 C. Moldoveanu, Gh. Zbancioc, G. Mangalagiu and I. Mangalagiu, Action of Cyclic Unsaturated Anhydride toward 4-R-Pyrimidines, The JCF – Fruhjahrssymposium 2006, 16–18 March, Konstanz–Germany, IBSN 3-86537-700-7, p. 119.
19 E. M. Barrall, Thermochim. Acta, 5 (1973) 577.

Received: December 10, 2007
Accepted: January 25, 2008

DOI: 10.1007/s10973-007-8918-6